Nano Today 55 (2024) 102141

Contents lists available at ScienceDirect

Nano Today

journal homepage: www.elsevier.com/locate/nanotoday

Anti-biofilm super-hydrophilic gel sensor for saliva glucose monitoring

Tingjun Chen [a], Jing Pang [b], Xinchuan Liu [a], Na Chen [a,c], Chenchen Wu [a,c], Yu Duan [a], Xuefu You [b], Qian Dou [a,c,*], Chao Yuan [d,**], Yanxiang Wang [b,**], Qing Dai [a,c]

[a] CAS Key Laboratory of Nanophotonic Materials and Devices, CAS Key Laboratory of Standardization and Measurement for Nanotechnology, National Center for Nanoscience and Technology, Beijing 100190, China
[b] Beijing Key Laboratory of Antimicrobial Agents, Institute of Medicinal Biotechnology, Chinese Academy of Medical Sciences and Peking Union Medical College, Beijing 100050, China
[c] Center of Materials Science and Optoelectronics Engineering, University of Chinese Academy of Sciences, Beijing 100049, China
[d] Department of Preventive Dentistry, Peking University School and Hospital of Stomatology, National Center for Stomatology, National Clinical Research Center for Oral Diseases, National Engineering Research Center of Oral Biomaterials and Digital Medical Devices, Beijing 100081, China

A R T I C L E I N F O

Keywords:
Saliva glucose
Non-invasive blood glucose monitoring
Anti-bacterial adhesion
Super-hydrophilic gel sensor
Wearable oral monitoring

A B S T R A C T

Accurate detection of saliva glucose levels is crucail for diagnosing diabetes and oral diseases. However, the complex bacterial environment in the oral cavity presents challenges, particularly in reducing sensor sensitivity due to bacterial adhesion. The excellent self-cleaning capabilities of super-hydrophilic materials make them one of the top choices. To surpass the limitations of traditional super-hydrophilic materials, a Spin coating-Plasma treatment-Coprecipitation treatment (SPC) strategy was implemented to develop a super-hydrophilic gel saliva glucose sensor. Surface-initiated polymerization was used to form phenylboric acid hydrogels for glucose binding. A spin-coated transition layer protects the hydrogel, while plasma treatment and co-precipitation methods create a super-hydrophilic surface, providing antibacterial properties. The sensor demonstrated a remarkable ability to reduced bacterial adhesion of the five oral pathogenic bacteria by over 95 %, and significantly inhibited biofilm formation of *Streptococcus pneumoniae* and *Streptococcus mitis* by 95.7 % and 96.7 %, respectively. Its detection limit of 3.04 mg/L meets the requirements for saliva glucose detection. Overall, the development of this super-hydrophilic gel sensor holds great promise for wearable oral monitoring devices, offering new opportunities in healthcare managing and monitoring.

Introduction

In the quest for non-invasive blood glucose monitoring, saliva glucose emerges as a pivotal biomarker due to its robust correlation with blood glucose levels, as evidenced by multiple studies [1–4]. This correlation underscores the potential of saliva glucose monitoring in clinical diagnostics. However, an upsurge in saliva glucose can catalyze the proliferation of oral pathogens, thereby escalating the risk of various oral diseases [5–7]. Consequently, real-time monitoring of saliva glucose concentration acquires paramount clinical relevance. The oral cavity, a reservoir of a diverse and complex microbial ecosystem, comprising approximately 700 bacterial species [8], poses a significant challenge for the deployment of oral wearable sensors. These bacteria can colonize the surfaces of sensors, leading to biofilm formation, which in turn impairs the sensitivity and durability of these devices [9–11]. Bacterial biofilm formation follows a multi-step dynamic process (Fig. 1) [12–14]. I) Initially, bacteria make contact with the material's surface, resulting in reversible bacterial adhesion. II) Subsequently, genes associated with biofilm formation are activated, leading to irreversible adherence of bacteria to the material's surface. III) As the biofilm matures, the bacteria organize into a highly structured microcolony. IV) Bacteria shed or are released from mature biofilms, reverting to a planktonic state, and have the potential to form new biofilms. Thus, during saliva glucose detection, a large number of bacteria will attach to the surface of the sensor to form biofilms, affecting the accuracy and reliability of the sensor [15–17].

In response to these challenges, the antifouling and anti-bacterial adhesion properties of materials have become a focus of research,

* Corresponding author at: CAS Key Laboratory of Nanophotonic Materials and Devices, CAS Key Laboratory of Standardization and Measurement for Nanotechnology, National Center for Nanoscience and Technology, Beijing 100190, China.
** Corresponding authors.
E-mail addresses: douq@nanoctr.cn (Q. Dou), chaoyuan@bjmu.edu.cn (C. Yuan), wangyanxiang@imb.pumc.edu.cn (Y. Wang).

https://doi.org/10.1016/j.nantod.2023.102141
Received 8 August 2023; Received in revised form 2 December 2023; Accepted 24 December 2023
Available online 11 January 2024

with studies indicating a positive correlation between these properties and the material's hydration level [18,19]. Super-hydrophilic materials, therefore, emerge as the preferred choice for combating these issues. Indeed, their ability to form hydration layers on their surfaces not only prevents bacterial contact but also facilitates self-cleaning through the removal of surface bacteria by water [20–22]. There are generally two approaches to achieving super-hydrophilic surfaces: one involves constructing rough structures on hydrophilic surfaces [23,24]. Li *et al.* utilized a hydrothermal synthesis method to create microscale rough structures on the surface of aluminum and its alloys, resulting in a super-hydrophilic surface [25]. The other approach involves introducing hydrophilic functional groups onto the surface [26,27]. An *et al.* grafted hyperbranched polyglycerol onto a polyamide thin film composite layer, resulting in the formation of a super-hydrophilic surface with excellent anti-fouling properties [28]. However, these approaches introduce complexities and challenges, such as the stability and durability of nanostructures and the homogeneity of hydrophilic surfaces.

This study introduces a novel sensor with a super-hydrophilic surface, specifically engineered to address the aforementioned challenges. Our research endeavors included: i) evaluate the sensor's capability to prevent bacterial adhesion, ii) verify the biofilm formation resistant ability of the sensor to the predominant bacteria at high saliva glucose levels, iii) evaluate the accuracy of the sensor for the saliva glucose determination. The findings reveal that the super-hydrophilic hydrogel sensor markedly reduces bacterial adhesion by over 95 % against five oral pathogenic bacteria and effectively inhibits biofilm formation. Furthermore, the sensor's detection limit of 3.04 mg/L aligns with the requisites for saliva glucose monitoring, showcasing its potential in clinical applications.

Experimental section

Reagents and instruments

3-Aminopropyltriethoxysilane (98 %) and polyethyleneimine (PEI , 99 %, M_w 1800) were sourced from Alfa Aesar Chemicals Co., Ltd. (3-Methacrylamidophenyl) boronic acid (PBA , 99.92 %, Ark Pharm, Inc.), N,N-Methylenebisacrylamide (BIS, 98 %, Sinopharm Chemical Reagent Co. Ltd.), acrylamide (AM, 99.0 %), tannic acid (TA), polyvinylpyrrolidone (PVP) were purchased from Macklin Biochemical Co., Ltd. 2,2-Dimethoxy-1,2-diphenylethanone (DMPA, 98.0 %, TCI Development Co., Ltd.), Carboxylated nanofiber cellulose (CNF-C, Qihong Technology Co., Ltd.), polyethyleneimine (bPEI, M_w 25000), Crystal violet was purchased from Innochem. Glucose, N,N-dimethylformamide, and maleic anhydride are all pure analytical reagents. Brain Heart Infusion (BHI) broth and agar used for bacterial cultures were sourced from Becton, Dickinson and Company. Film-tracer™ SYPRO® Ruby Biofilm Matrix Stain was purchased from Thermo Fisher Scientific Inc.

Saliva glucose level and anti-protein properties were tested by Quartz crystal microbalance (QCM 200, Stanford Research Systems). Reactive Ion Etching (ETCHLAB 200) was used for plasma treatment. The morphologies of the sensor surface were investigated using Scanning Electron Microscope (SEM, SU-8200). Hydrophilicity was measured using a fully automatic contact angle measuring instrument (DSA-100). X-ray Photoelectron Spectroscopy (XPS, ESCALAB250Xi) was used to determine the elemental composition of sensor surfaces. The external force applied during the sensor coating formation was achieved through a lab-built pressure film machine. Ultraviolet polymerization was performed using a UV lamp (wavelength $\lambda = 365$ nm and maximum power = 3 W). Spin coating of films was performed using a Spin-coater (KW-4B, Beijing SETCAS Electronics Co., Ltd.). The stained biofilm matrix imaging was performed on an IVIS® Spectrum in Vivo Imaging System (IVIS, PerkinElmer Inc.).

Surface modification of the QCM electrode

The preprocessing of chips followed the method outlined in our previous work. In short, the QCM chips were placed in a piranha solution (H_2SO_4 (98 % w/w) and H_2O_2 (30 % w/w) in a volume ratio of 7:3 and were ultrasonicated for 10 min, then rinsed with distilled water and dried with N_2. Subsequently, the chips were ultrasonicated in acetone, ethanol, then distilled water for 10 min respectively, then dried with N_2. The treated chips were placed in a mixture of 3-aminopropyl triethoxysilane and toluene (v/v 1:10) for 12 h, rinsed with ethanol and dried with N_2. Finally, the dried chips were immersed in a mixture of maleic anhydride (25 mL) and N,N-dimethylformamide (500 mg) for 12 h, rinsed with ethanol and dried with N_2 for further modification.

Preparation of PBA hydrogel (HPBA)

First, the chip's surface underwent modification through surface-initiated polymerization. PBA (17.2 mg), BIS (1.54 mg), AM (27.7 mg), and DMPA (2.56 mg) were added into 100 μL of DMSO to form the prepolymer. Then, 30 μL of the prepolymer was deposited on the processed chip under pressure to form a thin film with uniform thickness [29]. Finally, HPBA was obtained after placing the chips under ultraviolet light ($\lambda = 365$ nm) for 1 h. Then, the chips were rinsed with distilled water and dried with N_2 for future modification. The HPBA containing glucose-capturing unit PBA, AM, and BIS was used to

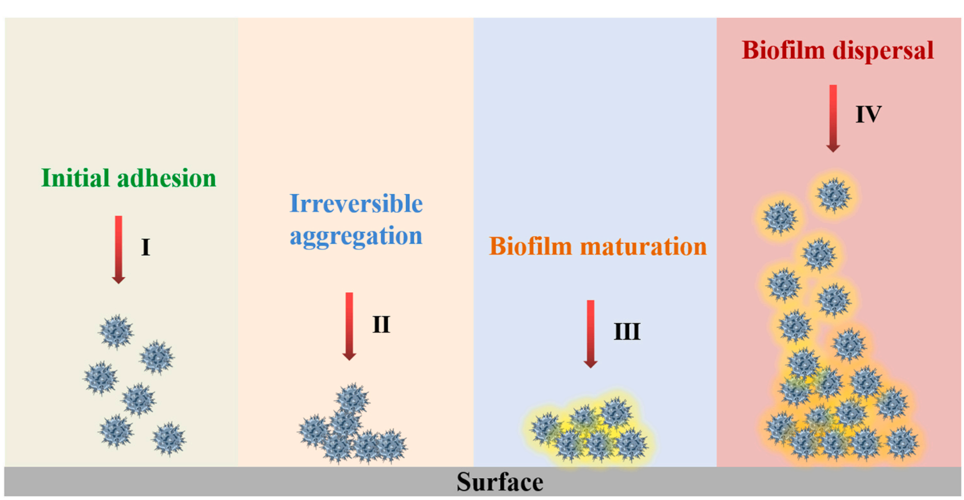

Fig. 1. The process by which bacteria form biofilms. I) initial adhesion, II) irreversible aggregation, III) biofilm maturation, and IV) biofilm dispersal.

construct the hydrogel framework, and as a free radical photoinitiator, DMPA was used to initiate the polymerization and the crosslinking of AM and BIS.

Preparation of CNF-C@bPEI/HPBA

A transition layer was modified on HPBA using spin coating. For this, CNF-C (2 g) was added into 40 mL of distilled water containing EDC (80 mg) and NHS (120 mg) and was allowed to react for 15 min. Next, PEI (2 g) was added and the mixture was stirred overnight with a magnetic stirrer. The obtained white floccules were centrifuged at high speed (10,000 rpm, 10 min), and the supernatant was removed. The pellet was then redispersed in 1 mL of ethanol to obtain the spin-coating solution. Finally, 50 μL of the spin coating solution was used to prepare CNF-C@bPEI/ HPBA using spin coating (low-speed: 500 rpm, 5 s, high-speed: 3000 rpm, 30 s), then the chips were rinsed with distilled water and dried with N_2.

Preparation of plasma-treated CNF-C@bPEI/HPBA

Plasma surface treatment technology can easily and effectively change the chemical composition and rough structure of the surfaces of materials. Plasma-treated CNF-C@bPEI/HPBA was obtained after treatment with O_2 plasma (O_2 flow rate: 20 sccm, time: 5 min, power: 200 W). The plasma-treated chips were then rinsed with distilled water and dried with N_2. This step significantly increases the free energy of the Plasma-treated CNF-C@bPEI/HPBA surface and reduces the surface wetting angle, thus achieving the super-wettability state.

Preparation of coprecipitation-treated CNF-C@bPEI/HPBA

Due to the high energy of polar groups, the hydrophobic polymer chain can embed these groups on the inside through rearrangement, resulting in a "hydrophobic recovery" phenomenon. Therefore, we prolonged the super-hydrophilic aging through mild coprecipitation treatment. TA (20 mg), PEI (5 mg), and PVP (50 mg) were dissolved in 30 mL of distilled water by ultrasonication to obtain the coprecipitation solution. Coprecipitation-treated CNF-C@bPEI/HPBA chips were obtained by placing Plasma-treated CNF-C@bPEI/HPBA chips face up in the coprecipitation solution for 12 h. Finally, the chips were rinsed with distilled water and dried with N_2 for subsequent testing.

QCM measurements

Coprecipitation-treated CNF-C@bPEI/HPBA were placed in the QCM flow cell. Phosphate buffer solution (PBS) (0.1 mol/L) was continuously pumped into the flow cell at an appropriate flow rate under the action of a peristaltic pump, and the change of the chip frequency (ΔF) was monitored in real-time by the QCM data acquisition software. When ΔF was stable, we investigated the sensitivity of glucose detection and antifouling performance.

Saliva samples

The collection of saliva samples was supported by the "Early identification, early diagnosis, and cutting point of diabetes risk factors" program (2016YFC1305700). Saliva samples were collected from ordinary urban and rural residents in Yancheng, Jiangsu Province, China, who were between 18 and 65 years old and had no history of mental illness. Informed consent was obtained from all participants and experiments were approved by the Medical ethics committee of Jiangsu Provincial Center for Disease Control and Prevention (JSJK2017-B003–02), China.

Saliva collection and processing

Five males and five females between the ages of 20 and 40, who were restricted to glucose drinks 1 h before sample collection were selected for the study. Subjects drank 200 mL of water 30 min before collecting the saliva sample.

A saliva collector was used to collect non-irritating saliva. During sample collection, subjects relaxed, sat upright, tilted their heads slightly, and spat saliva naturally into the sterile disposable centrifuge tube. A total of 15 mL sample was collected from each subject.

The collected saliva samples were divided into 6 groups for each subject. Different concentrations of glucose were added to each group's samples (0 mg/L, 50 mg/L, or 100 mg/L glucose, two groups for each concentration). Then, the saliva samples with the same concentration were stored at room temperature for 1 h or 2 h. The processed saliva samples were stored at –80 °C until the oral flora analysis. The specific operation flow chat is described in Fig. S1.

Antibacterial measurements

All bacterial strains used in this study were obtained from the Collection Center of Pathogen Microorganisms of Chinese Academy of Medical Sciences (CAMS-CCPM-A), China. Widely distributed bacteria in saliva and daily environment, *Staphylococcus epidermidis* (*S. epidermidis*) ATCC 12228, *Streptococcus mutans* (*S. mutans*) ATCC 25715, *Streptococcus pneumoniae* (*S. pneumoniae*) ATCC 51916, *Streptococcus mitis* (*S. mitis*) ATCC 49456, *Streptococcus oralis* (*S. oralis*) ATCC 35037 were chosen for the adhesion experiments and were stored at –80 °C. These bacteria were incubated by streaking on brain heart infusion (BHI) agar plates to make fresh overnight cultures. Then, one colony of each strain was inoculated into 10 mL of BHI broth and incubated for 24 h at 37 °C except for *S. mutans* which required a longer incubation time of 48 h. *S. mitis*, *S. pneumoniae*, and *S. oralis* were inoculated anaerobically. Bacteria were then harvested by centrifugation (2400 *g*) for 10 min, washed twice in sterile PBS, and their concentration was adjusted to 1×10^7 CFU/mL in sterile PBS for the adhesion experiments.

The different surfaces were placed in 2 mL bacterial suspension in 6-well cell culture plates and were incubated for 3 h at 37 °C. After incubation, samples were picked up with sterile forceps, mildly rinsed with sterile PBS to remove the loosely adherent bacteria, and soaked in 2 mL of sterile PBS in new 6-well cell culture plates. To quantify viable adherent bacteria, the plates were subjected to a 30 s sonication, and 10 μL serially diluted samples were drop-plated on BHI agar plates in triplicates. The plates were incubated at 37 °C for 24 or 48 h and the colony-forming units (CFU) were counted. The results were expressed as CFU/mL.

To investigate the bacterial cell morphology on different surfaces, one sample from each group was fixed with 2.5 wt% glutaraldehyde for 24 h. Then, they were passed through an ethanol gradient for dehydration, dried, coated with gold, and observed using SEM.

Biofilm adhesion measurements

S. mitis, S. pneumoniae, and *S. oralis* were cultured anaerobically overnight at 37 °C. The different sensors were immersed in 2 mL of 1:100 diluted overnight inoculums in 6-well cell culture plates to form biofilms for 24 h. Samples were then mildly washed with PBS 3 times to remove planktonic bacteria for the subsequent study.

Drop plate method was used for determining viable counts of bacteria in biofilm as described above. For fluorescence staining, the biofilm matrix was quantified by staining with Filmtracer SYPRO Ruby Biofilm Matrix Stain. In the crystal violet staining, biofilms were fixed at 60 °C, then 1 mL of 0.06 % crystal violet was added to each well, stained for 5 min, and crystal violet was removed by repeated washing with water.

Results and discussion

Synthesis of the super-hydrophilic gel sensor

The SPC strategy was employed to design and construct a super-hydrophilic coating on the PBA hydrogel, aiming to prevent biological contamination on the sensor surface and ensuring accurate glucose detection in saliva. The specific design steps are outlined as follows (Fig. 2a): i) initiating the polymerization reaction through ultraviolet irradiation to form a glucose-responsive hydrogel on the chips (HPBA). ii) spin-coating a transition layer on the surface of HPBA (CNF-C@bPEI/HPBA) to shield it from direct bombardment during plasma treatment, iii) the plasma treatment etches the material, introduces hydrophilic groups on the surface, and form a micro-nano rough structure, resulting in a super-hydrophilic state (Plasma-treated CNF-C@bPEI/HPBA), iv) delaying and improving the "hydrophobicity recovery" of super-hydrophilic materials through co-precipitation (Coprecipitation-treated CNF-C@bPEI/HPBA), thus further enhancing the hydrophilic properties. The introduction of the transition layer not only enhances the hydrophilic functional groups and permeability of the surface but also protects the stability of the underlying hydrogel. Plasma treatment addresses the issue of non-uniform hydrophilic functional group distribution while preserving the intrinsic substrate properties. Co-precipitation method further enhances the stability of the super-hydrophilic coating, resulting in a 10-fold improvement in its super-hydrophilic stability. For a more detailed description of the construction process and characterization results of the superhydrophilic hydrogel sensor, please refer to the Supplementary Material. (Table S1, Fig. S2-6). Based on this, when the super-hydrophilic gel sensor detects saliva glucose, the hydration on the sensor surface can prevent bacterial contact and biofilm formation, and ultimately safeguards the sensor from biocontamination.

Bacterial adhesion-preventing properties of super-hydrophilic gel sensor

To compare the effect of the different modifications, antibacterial experiments were conducted at various stages of the sensor (Fig. 3a). *Staphylococcus* and *Streptococcus,* which are relatively abundant in the oral cavity were taken as examples to assess the impact of bacteria on different surface sensors (Fig. 3b). The results showed that the super-hydrophilic coating displayed a significant anti-adhesion effect on all five bacterial strains when compared to the hydrogel coating. The anti-adhesion efficacies for *S. epidermidis*, *S. mutans*, *S. pneumoniae, S. mitis* and *S. oralis* were increased by 96.3 ± 0.30 %, 98.4 ± 0.31 %, 96. 8 ± 0.28 %, 99.9 ± 0.02 % and 95.2 ± 1.18 %, respectively (Table S2, Fig. S7).

Biofilm formation resistance properties of super-hydrophilic gel sensor

Taking into account the high-glucose environment in the oral cavity where the sensor is placed, we conducted further investigations using metagenomic sequencing to explore the oral bacterial species most influenced by elevated saliva glucose levels. The specific operation protocol is described in Fig. S1. *Streptococci,* in particular *S. pneumoniae, S. mitis,* and *S. oralis* exhibited the highest increase in relative abundance in the treatment of glucose. Notably, their relative abundance displayed a time- and dose-dependent rise (Fig. 4a). Consequently, these strains were selected for evaluating the sensor's anti-biofilm capacity.

Subsequently, the biofilm-forming resistance capacity of the different surfaces was evaluated. After 24 h of biofilm formation of *S. pneumoniae*, *S. mitis,* and *S. oralis*, bacteria counts were recored on the different surfaces. As expected, *S. pneumoniae, S. mitis*, and *S. oralis* attached to surface coprecipitation-treated CNF-C@bPEI/HPBA were reduced by 95.8 ± 0.74 %, 96.7 ± 0.65 %, and 76.8 ± 6.51 %, respectively (Fig. 4b). This observation was further supported by SEM analysis, which consistently demonstrated a suppression of biofilm formation on the coprecipitation-treated CNF-C@bPEI/HPBA surface.

Given its higher abundance, *S. mitis* was selected for visualization using crystal violet and Filmtracer SYPRO Ruby Biofilm Matrix Stain for staining the biofilm mass and extracellular matrix, respectively. The intensity of crystal violet visually observed and fluorescence detected using the IVIS Spectrum on the coprecipitation-treated coating was remarkable reduced (Fig. 4c), providing additional confirmation of its resistance to both bacterial adhesion and extracellular matrix formation

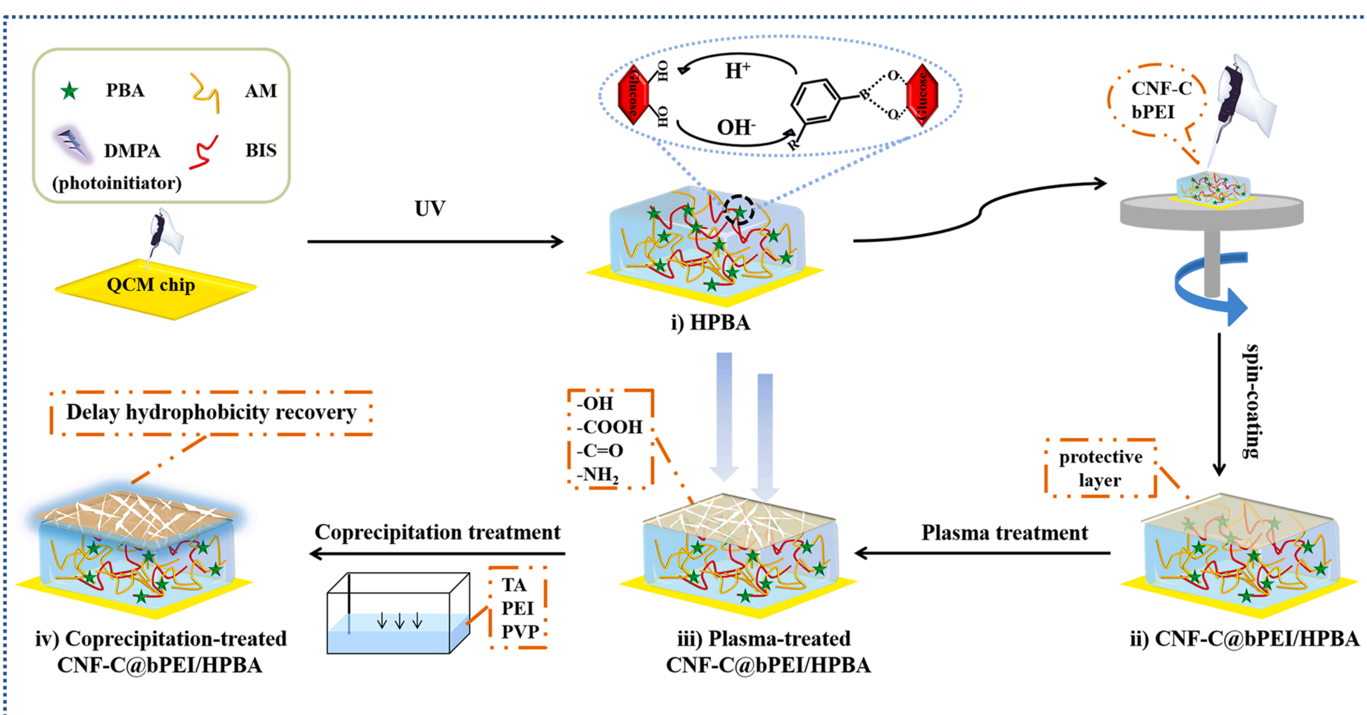

Fig. 2. The schematic illustration of the synthesis of super-hydrophilic gel sensor.

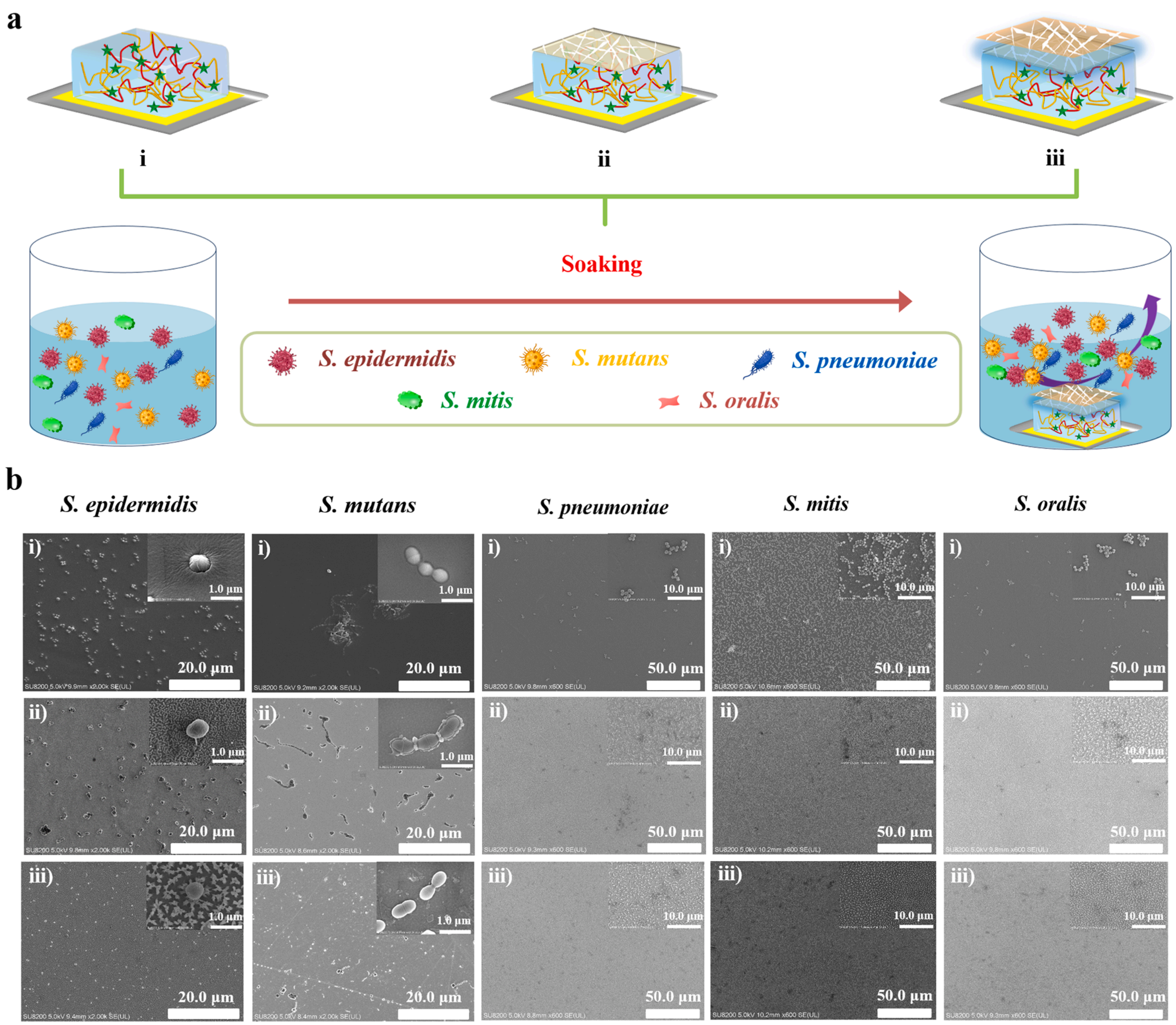

Fig. 3. a) Effects of bacteria on different modification sensors: i) HPBA, ii) Plasma-treated CNF-C@bPEI/HPBA, iii) Coprecipitation-treated CNF-C@bPEI/HPBA. b) SEM images of bacterial adsorption on sensors. (i) HPBA, (ii) Plasma-treated CNF-C@bPEI/HPBA, (iii) Coprecipitation-treated CNF-C@bPEI/HPBA.

in biofilms.

Furthermore, we explored the sensor's adsorption capacity for oral proteins in Table S4 and Fig. S8, which also confirmed the excellent antifouling performance of the super-hydrophilic gel sensor.

Saliva glucose detection by super-hydrophilic gel sensors

The super-hydrophilic sensor was used to detect saliva glucose, and its sensitivity was evaluated by QCM. First, the ΔF of the Coprecipitation-treated CNF-C@bPEI/HPBA remainede stable between –1.3 and 1.5 Hz within 14 h, indicating reliable detection of saliva glucose detection (Fig. 5a). Next, different concentrations of glucose were detected in the range of 0–200 mg/L (Fig. 5b). The absolute value of ΔF increased rapidly with the rise in glucose concentration, which confirmed the sensor's excellent response to glucose. In the enlarged plot at the upper right corner of Fig. 5b, there was no significant change at baseline when glucose concentration was 0 mg/L. The "baseline" corresponding to the glucose solution gradually decreased, representing that the sensor was constantly adsorbing glucose molecules, rather than the baseline drift. Moreover, as the combination of boric acid and glucose is affected by pH, we tested saliva glucose within the physiological pH range of saliva (Fig. 5d). As expected, ΔF increases with increasing pH, facilitating the binding of boric acid molecules to glucose molecules in the hydrogel network. In addition, a strong linear relationship was observed between the concentration of glucose and the response within the range of 0 to 60 mg/L under different pH conditions (Fig. 5e). Moreover, at a pH value of 7.5 and a glucose concentration range of 0 to 60 mg/L, the detection limit was 3.04 mg/L determined by the 3 SD/N method (SD is the standard deviation and N is the slope of linear regression equation). Additionally, the corresponding linear correlation coefficients increased with pH, reaching 0.9274, 0.9201, and 0.9525 at pH values of 6.8, 7.3, and 7.5, respectively.

After that, in order to simulate the low-biocontamination performance of the super-hydrophilic gel sensor in detecting glucose in real saliva samples, we added different concentrations of glucose to 50 % saliva (V_{PBS}:V_{Saliva}=1:1) (Fig. 5c). The results show an obvious decrease in ΔF with the increase in glucose concentration.

By comparing the detection performance of various saliva glucose

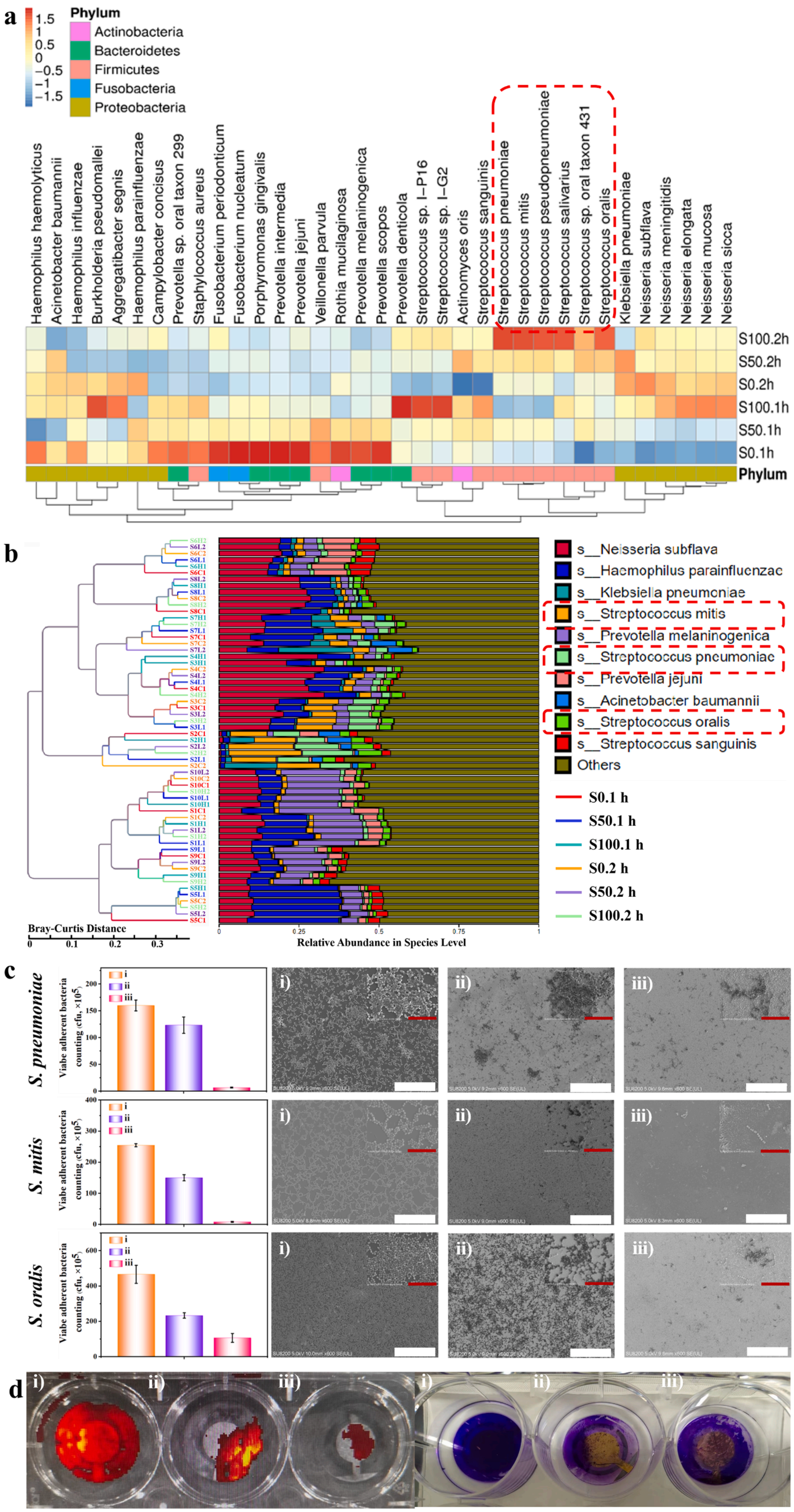

(caption on next page)

Fig. 4. The relationship between saliva glucose and oral bacteria was analyzed by metagenomic sequencing. a) The inter-species analysis results of bacteria. b) The relative abundance and individual differences of the top 10 bacterial species in total quantity. c) SEM images of the effect of coating on bacteria biofilms: (i) HPBA, (ii) Plasma-treated CNF-C@bPEI/HPBA, and (iii) Coprecipitation-treated CNF-C@bPEI/HPBA. Red scale bar: 10 µm, white scale bar: 50 µm. d) IVIS Spectrum images and crystal violet staining images of the effect of coating on *S. mitis* biofilm: (i) HPBA, (ii) Plasma-treated CNF-C@bPEI/HPBA, and (iii) Coprecipitation-treated CNF-C@bPEI/HPBA.

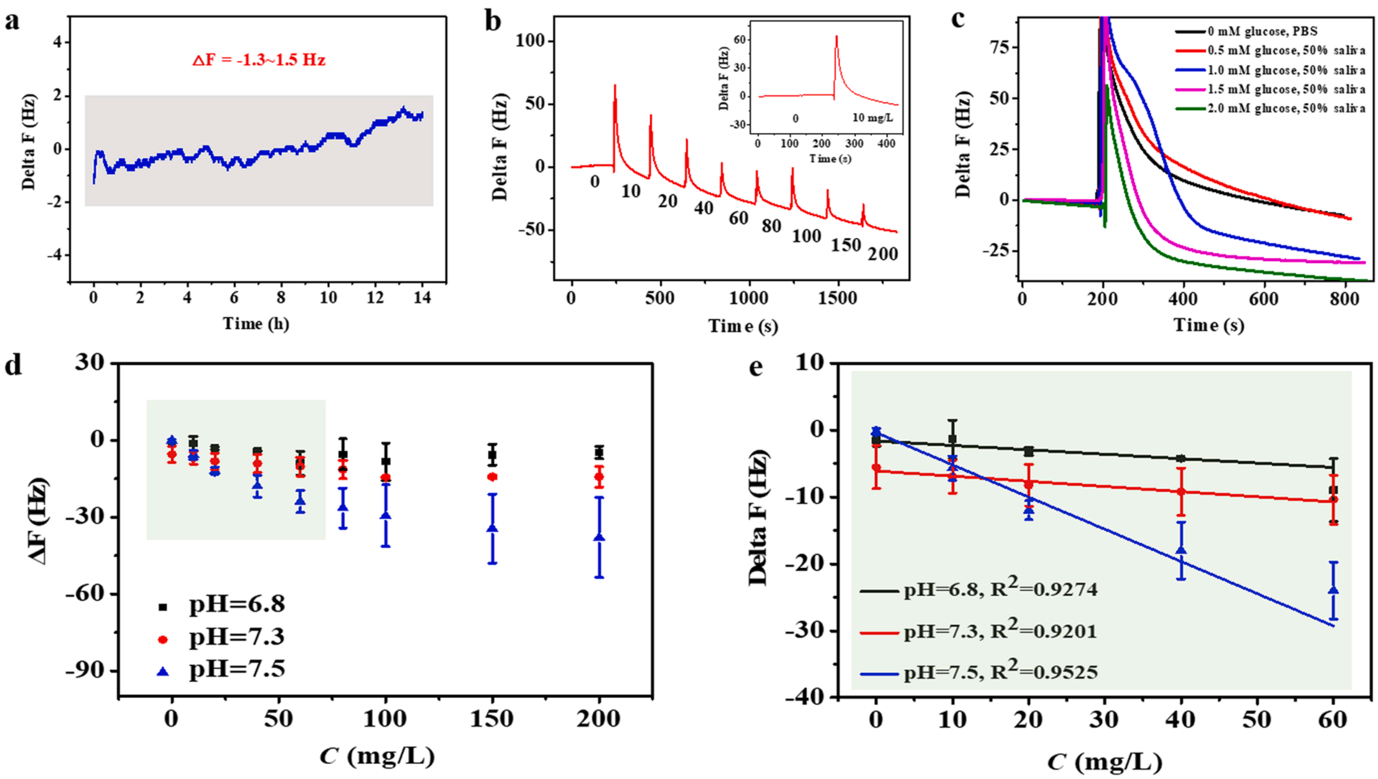

Fig. 5. a) Stability test of super-hydrophilic gel QCM sensor. b) Response of the super-hydrophilic sensor to different concentrations of glucose. Inset: response of the superhydrophilic sensor to 0 and 10 mg/L glucose. c) Response of the super-hydrophilic sensor to different concentrations of glucose in 50 % saliva. d) Response of the super-hydrophilic sensor to different concentrations of glucose at different pH values (6.8–7.5), data are representative of three independent measurements. e) Response trend of the super-hydrophilic sensor to different concentrations of glucose at different pH values (6.8–7.5), data are representative of three independent measurements.

sensors in Table S5, the super-hydrophilic gel sensor shows comparable sensitive detection ability of saliva glucose.

Conclusions

To mitigate the adverse impact of the oral environment on saliva glucose sensors performance, we have conducted in-depth explorations in the construction of a novel sensor, contributed to the emergence of a super-hydrophilic hydrogel sensor. Endowed with special hydration ability by super-hydrophilic coating on the sensor surface, it exhibits superior resistance to bacterial adhesion and biofilm formation. This feature significantly improves the accuracy of the saliva glucose sensor, with a detection limit of 3.04 mg/L, which met the needs of saliva glucose detection. Therefore, the successful development of this super-hydrophilic gel saliva glucose sensor is notably significant for the fields of oral health monitoring and management. Additionally, it introduces a new strategy improving the reliability and longevity of biosensors.

CRediT authorship contribution statement

Chen Na: Validation. **Liu Xinchuan:** Validation. **Pang Jing:** Data curation, Investigation, Software, Validation. **Dou Qian:** Conceptualization, Data curation, Project administration, Software, Supervision, Validation, Visualization, Writing – review & editing. **You Xuefu:** Validation. **Duan Yu:** Validation. **Wu Chenchen:** Validation. **Chen Tingjun:** Conceptualization, Data curation, Formal analysis, Investigation, Methodology, Software, Validation, Visualization, Writing – original draft. **Dai Qing:** Funding acquisition, Project administration, Writing – review & editing. **Wang Yanxiang:** Conceptualization, Funding acquisition, Methodology, Project administration, Supervision, Visualization, Writing – review & editing. **Yuan Chao:** Conceptualization, Methodology, Project administration, Funding acquisition, Writing – review & editing.

Declaration of Competing Interest

The authors declare that they have no known competing financial interests or personal relationships that could have appeared to influence the work reported in this paper.

Data Availability

Data will be made available on request.

Acknowledgements

This work was supported by the National Key R&D Program of China (grant number 2022YFE0118300), the Special scientific research project for Capital Hygiene Development focused on the research of "establishment of a mathematical model for saliva glucose and blood glucose, development of glucose-sensitive anti-fouling nanoprobes" (2022–2-5042), the National Natural Science Foundation of China (grant numbers 51925203 & 32141003 & U2032206), the CAMS Initiative for Innovative Medicine (2021-1-I2M-030, China), and the Strategic Priority Research Program of Chinese Academy of Sciences (grant number XDB36000000).

Appendix A. Supporting information

Supplementary data associated with this article can be found in the online version at doi:10.1016/j.nantod.2023.102141.

References

[1] M. Dhanya, S. Hegde, Niger. J. Clin. Pract. 19 (2016) 486–490.
[2] Y. Du, W. Zhang, M.L. Wang, J. Diabetes Sci. Technol. 10 (2016) 1344–1352.
[3] J. Wang, L. Xu, Y. Lu, K. Sheng, W. Liu, C. Chen, Y. Li, B. Dong, H. Song, Anal. Chem. 88 (2016) 12346–12353.
[4] R.S. Malon, S. Sadir, M. Balakrishnan, E.P. Córcoles, BioMed. Res. Int. 2014 (2014) 962903.
[5] A.C.M. Brito, I.M. Bezerra, M.H.S. Borges, Y.W. Cavalcanti, L.F.D. Almeida, Biofouling 37 (2021) 615–625.
[6] H. Alqaderi, M. Tavares, M. Hartman, J.M. Goodson, J. Dent. Res. 95 (2016) 1387–1393.
[7] W.G. Wade, Periodontology 2000 (86) (2021) 113–122.
[8] N.B. Arweiler, L. Netuschil, Adv. Exp. Med. Biol. 902 (2016) 45–60.
[9] J. Xu, H. Lee, Chemosensors 8 (2020) 66.
[10] P.H. Lin, B.R. Li, Analyst 145 (2020) 1110–1120.
[11] N. Liu, Z. Xu, A. Morrin, X.J.A.M. Luo, Anal. Methods 11 (2019) 702–711.
[12] F. Ghilini, D.E. Pissinis, A. Miñán, P.L. Schilardi, C. Diaz, ACS Biomater. Sci. Eng. 5 (2019) 4920–4936.
[13] K. Sauer, P. Stoodley, D.M. Goeres, L. Hall-Stoodley, M. Burmølle, P.S. Stewart, T. Bjarnsholt, Nat. Rev. Microbiol. 20 (2022) 608–620.
[14] S. Singh, S. Datta, K.B. Narayanan, K.N. Rajnish, J. Genet. Eng. Biotechn. 19 (2021) 140.
[15] D. Chan, J.C. Chien, E. Axpe, L. Blankemeier, S.W. Baker, S. Swaminathan, V. A. Piunova, D.Y. Zubarev, C.L. Maikawa, A.K. Grosskopf, J.L. Mann, H.T. Soh, E. A. Appel, Adv. Mater. 34 (2022) e2109764.
[16] N. Wisniewski, M. Reichert, Colloids Surf. B, Biointerfaces 18 (2000) 197–219.
[17] N. Wisniewski, F. Moussy, W.M. Reichert, Fresenius' J. Anal. Chem. 366 (2000) 611–621.
[18] C.C. Chang, K.W. Kolewe, Y. Li, I. Kosif, B.D. Freeman, K.R. Carter, J.D. Schiffman, T. Emrick, Adv. Mater. Interfaces 3 (2016) 1500521.
[19] B. Li, P. Jain, J. Ma, J.K. Smith, Z. Yuan, H.C. Hung, Y. He, X. Lin, K. Wu, J. Pfaendtner, S. Jiang, Sci. Adv. 5 (2019) eaaw9562.
[20] Z. Zhu, S. Zheng, S. Peng, Y. Zhao, Y. Tian, Adv. Mater. 29 (2017) 1703120.
[21] S. Chen, L. Li, C. Zhao, J.J.P. Zheng, Polymers 51 (2010) 5283–5293.
[22] P.J. Molino, D. Yang, M. Penna, K. Miyazawa, B.R. Knowles, S. MacLaughlin, T. Fukuma, I. Yarovsky, M.J.J.An Higgins, ACS nano 12 (2018) 11610–11624.
[23] X. Liu, J. He, Langmuir 25 (2009) 11822–11826.
[24] J. Yang, Z. Zhang, X. Men, X. Xu, X. Zhu, X. Zhou, Q. Xue, J. Colloid Interf. Sci. 366 (2012) 191–195.
[25] L. Li, Y. Zhang, J. Lei, J. He, R. Lv, N. Li, F. Pan, Chem. Commun. 50 (2014) 7416–7419.
[26] J. Fang, A. Kelarakis, L. Estevez, Y. Wang, R. Rodriguez, E.P. Giannelis, J. Mater. Chem. 20 (2010) 1651–1653.
[27] T. Han, Z. Ma, D. Wang, ACS Macro Lett. 10 (2021) 354–358.
[28] X. An, K. Zhang, Z. Wang, Q.V. Ly, Y. Hu, C. Liu, J. Membr. Sci. 612 (2020) 118417.
[29] Q. Dou, Z. Zhang, Y. Wang, S. Wang, D. Hu, Z. Zhao, H. Liu, Q. Dai, ACS Appl. Mater. Interfaces. 12 (2020) 34190–34197.